

1 Running head: **Phylogenomics of *Triturus* newts**

2

3 **Phylogenomics of the adaptive radiation of *Triturus* newts supports gradual ecological**
4 **niche expansion towards an incrementally aquatic lifestyle**

5

6 B. Wielstra^{a,b,c,d,1,*}, E. McCartney-Melstad^{a,e,1}, J.W. Arntzen^c, R.K. Butlin^{b,f}, H.B. Shaffer^{a,e}

7

8 ^a *Department of Ecology and Evolutionary Biology, University of California, Los Angeles,*
9 *CA 90095, USA.*

10 ^b *Department of Animal and Plant Sciences, University of Sheffield, S10 2TN Sheffield, UK.*

11 ^c *Naturalis Biodiversity Center, 2300 RA Leiden, The Netherlands.*

12 ^d *Institute of Biology Leiden, Leiden University, 2300 RA, Leiden, The Netherlands.*

13 ^e *La Kretz Center for California Conservation Science, Institute of the Environment and*
14 *Sustainability, University of California, Los Angeles, CA 90095, USA.*

15 ^f *Department of Marine Sciences, University of Gothenburg, Gothenburg 405 30, Sweden.*

16 ¹ *These authors contributed equally to this work.*

17 ** Corresponding author; e-mail: ben.wielstra@naturalis.nl*

18 **Abstract**

19 Newts of the genus *Triturus* (marbled and crested newts) exhibit substantial variation in the
20 number of trunk vertebrae (NTV) and a higher NTV corresponds to a longer annual aquatic
21 period. Because the *Triturus* phylogeny has thwarted resolution to date, the evolutionary
22 history of NTV, annual aquatic period, and their potential coevolution has remained unclear.
23 To resolve the phylogeny of *Triturus*, we generated a c. 6,000 transcriptome-derived marker
24 data set using a custom target enrichment probe set, and conducted phylogenetic analyses
25 using: 1) data concatenation with RAxML, 2) gene-tree summary with ASTRAL, and 3)
26 species-tree estimation with SNAPP. All analyses produce the same, highly supported
27 topology, despite cladogenesis having occurred over a short timeframe, resulting in short
28 internal branch lengths. Our new phylogenetic hypothesis is consistent with the minimal
29 number of inferred changes in NTV count necessary to explain the diversity in NTV observed
30 today. Although a causal relationship between NTV, body form, and aquatic ecology has yet
31 to be experimentally established, our phylogeny indicates that these features have evolved
32 together, and suggest that they may underlie the adaptive radiation that characterizes *Triturus*.

33

34 **Keywords:** morphology; phylogeny; sequence capture; systematics; target enrichment;
35 transcriptome

36 **1. Introduction**

37 Accurately retracing the evolution of phenotypic diversity in adaptive radiations requires
38 well-established phylogenies. However, inferring the true branching order in adaptive
39 radiations is hampered by the short time frame over which they typically unfold, which
40 provides little opportunity between splitting events for phylogenetically informative
41 substitutions to become established (resulting in low phylogenetic resolution; Philippe et al.,
42 2011; Whitfield and Lockhart, 2007) and fixed (resulting in incomplete lineage sorting and
43 discordance among gene-trees; Degnan and Rosenberg, 2006; Pamilo and Nei, 1988; Pollard
44 et al., 2006). Resolving the phylogeny of rapidly multiplying lineages becomes even more
45 complicated the further back in time the radiation occurred, because the accumulation of
46 parallel substitutions along terminal branches can lead to long-branch attraction (Felsenstein,
47 1978; Swofford et al., 2001). A final impediment is reticulation between closely related (and
48 not necessarily sister-) species through past or ongoing hybridization, resulting in additional
49 gene-tree/species-tree discordance (Kutschera et al., 2014; Leaché et al., 2014; Mallet et al.,
50 2016).

51 Phylogenomics, involving the consultation of a large number of markers spread
52 throughout the genome, has proven successful in resolving both recent (e.g. Giarla and
53 Esselstyn, 2015; Leaché et al., 2016; Léveillé-Bourret et al., 2018; Meiklejohn et al., 2016;
54 Nater et al., 2015; Scott et al., 2018; Shi and Yang, 2018) and more ancient (e.g. Crawford et
55 al., 2012; Irisarri and Meyer, 2016; Jarvis et al., 2014; McCormack et al., 2012; Song et al.,
56 2012) evolutionary radiations. The appeal of greatly increasing the amount of data available
57 for any given phylogenetic problem is that it often (but not always; see Philippe et al., 2011)
58 provides informative characters to resolve short branches in the tree of life. Advances in
59 laboratory and sequencing techniques, bioinformatics, and tree-building methods all facilitate
60 phylogenetic reconstruction based on thousands of homologous loci for a large number of

61 individuals, and promise to help provide the phylogenetic trees necessary to interpret the
62 evolution of eco-morphological characters involved in adaptive radiations (Alföldi et al.,
63 2011; Stroud and Losos, 2016). In this study, we conduct a phylogenomic analysis of an
64 adaptive radiation that moderately-sized multilocus nuclear DNA datasets (Arntzen et al.,
65 2007; Espregueira Themudo et al., 2009; Wielstra et al., 2014) have consistently failed to
66 resolve: the Eurasian newt genus *Triturus* (Amphibia: Urodela: Salamandridae), commonly
67 known as the marbled and crested newts.

68 One of the most intriguing features of *Triturus* evolution is the correlation between
69 certain aspects of their ecology and the number of trunk vertebrae (NTV; Fig. 1). Species
70 characterized by a higher modal NTV (which translates into a more elongate body build with
71 proportionally shorter limbs) are associated with a more aquatic lifestyle. Empirically, the
72 number of months a *Triturus* species spends in the water (defined at the population level as
73 the peak date of emigration, leaving a breeding pond, minus the peak in immigration,
74 entering it) roughly equals NTV minus 10 (Arntzen, 2003; Arntzen and Wallis, 1999;
75 Slijepčević et al., 2015). The intrageneric variation in NTV shown by *Triturus*, ranging from
76 12 to 17, is unparalleled in the family Salamandridae (Arntzen et al., 2015; Lanza et al., 2010)
77 and a causal relationship between NTV expansion and an increasingly aquatic lifestyle has
78 been presumed, but never adequately placed into a phylogenetic comparative analysis
79 (Arntzen, 2003; Arntzen et al., 2015; Arntzen and Wallis, 1999; Govedarica et al., 2017;
80 Slijepčević et al., 2015; Urošević et al., 2016; Vukov et al., 2011; Wielstra and Arntzen,
81 2011). A well-established *Triturus* species-tree is required to accurately retrace NTV
82 evolution and assess the concordance between aquatic lifestyle and NTV across the genus.

83 Our goal is to obtain a genome-enabled phylogeny for *Triturus* and use it to reconstruct
84 the eco-morphological evolution of NTV and aquatic/terrestrial ecology across the genus. As
85 the large size of salamander genomes hampers whole-genome sequencing (but see Elewa et

86 al., 2017; Nowoshilow et al., 2018; Smith et al., 2018), we employ a genome-reduction
87 approach in which we capture and sequence a set of transcriptome-derived markers using
88 target enrichment, an efficient technique that affords extremely high resolution at multiple
89 taxonomic levels (Abdelkrim et al., 2018; Bi et al., 2012; Bragg et al., 2016; Gnirke et al.,
90 2009; McCartney-Melstad et al., 2016; McCartney-Melstad et al., 2018). Using data
91 concatenation (with RAxML), gene-tree summarization (with ASTRAL) and species-tree
92 estimation (with SNAPP), we fully resolve the *Triturus* phylogeny and place the extreme
93 body shape and ecological variation observed in this adaptive radiation into an evolutionary
94 context.

95

96 **2. Materials and Methods**

97

98 *2.1 Target capture array design*

99 Nine *Triturus* newts (seven crested and two marbled newt species) and one banded newt
100 (*Ommatotriton*) were subjected to transcriptome sequencing. Transcriptome assemblies for
101 each species were generated using Trinity v2.2.0 (Grabherr et al., 2011), clustered at 90%
102 using usearch v9.1.13 (Edgar, 2010), and subjected to reciprocal best blast hit analysis (Bork
103 et al., 1998; Camacho et al., 2009; Tatusov et al., 1997) to produce a set of *T. dobrogicus*
104 transcripts (the species with the highest quality transcriptome assembly) that had putative
105 orthologues present in the nine other transcriptome assemblies. These transcripts were then
106 annotated using blastx to *Xenopus tropicalis* proteins, retaining one annotated transcript per
107 protein. We attempted to discern splice sites in the transcripts, as probes spanning splice
108 boundaries may perform poorly (Neves et al., 2013), by mapping transcripts iteratively to the
109 genomes of *Chrysemys picta* (Shaffer et al., 2013), *X. tropicalis* (Hellsten et al., 2010),
110 *Nanorana parkerii* (Sun et al., 2015) and *Rana catesbeiana* (Hammond et al., 2017). A single

111 exon ≥ 200 bp and ≤ 450 bp was retained for each transcript target. To increase the ability of
112 the target set to capture markers across all *Triturus* species, orthologous sequences from
113 multiple species were included for targets with $> 5\%$ sequence divergence from *T.*
114 *dobrogicus* (Bi et al., 2012). We generated a target set of 7,102 genomic regions for a total
115 target length of approximately 2.3 million bp. A total of 39,143 unique RNA probes were
116 synthesized as a MyBaits-II kit for this target set at approximately 2.6X tiling density by
117 Arbor Biosciences (Ann Arbor, MI, Ref# 170210-32). A detailed outline of the target capture
118 array design process is presented in Supplementary Text S1.

119

120 2.2 Sampling scheme

121 We sampled 23 individual *Triturus* newts (Fig. 2; Supplementary Table S1) for which tissues
122 were available from previous studies (Wielstra et al., 2017a; Wielstra et al., 2017b; Wielstra
123 et al., 2013). Because the sister-group relationship between the two marbled and seven
124 crested newts is well established (Fig. 1), while the relationships among the crested newt
125 species have defied resolution, we sampled the crested newt species more densely, including
126 three individuals per species to include intraspecific differentiation and to avoid misleading
127 phylogenies resulting from single exemplar sampling (Spinks et al., 2013). Because *Triturus*
128 species show introgressive hybridization at contact zones (Arntzen et al., 2014), we aimed to
129 reduce the impact of interspecific gene flow by only including individuals that originate away
130 from hybrid zones and have previously been interpreted as unaffected by interspecific genetic
131 admixture (Wielstra et al., 2017a; Wielstra et al., 2017b). The reality of phylogenetic
132 distortion by interspecific gene flow was underscored in a test for the phylogenetic utility of
133 the transcripts used for marker design which included a genetically admixed individual
134 (details in Supplementary Text S1).

135

136 *2.3 Laboratory methods*

137 DNA was extracted from samples using a salt extraction protocol (Sambrook and Russell,
138 2001), and 10,000ng per sample was sheared to approximately 200bp-500bp on a BioRuptor
139 NGS (Diagenode) and dual-end size selected (0.8X-1.0X) with SPRI beads. Dual-indexed
140 libraries were prepared from 375-2000ng of size selected DNA using KAPA LTP library
141 prep kits (Glenn et al., 2017). These libraries were pooled (with samples from other projects)
142 into batches of 16 samples at 250ng per sample (4,000ng total) and enriched in the presence
143 of 30,000ng of c0t-1 repetitive sequence blocker (McCartney-Melstad et al., 2016) derived
144 from *T. carnifex* (casualties from a removal action of an invasive population (Meilink et al.,
145 2015)) by hybridizing blockers with libraries for 30 minutes and probes with
146 libraries/blockers for 30 hours. Enriched libraries were subjected to 14 cycles of PCR with
147 KAPA HiFi HotStart ReadyMix and pooled at an equimolar ratio for 150bp paired-end
148 sequencing across multiple Illumina HiSeq 4000 lanes (receiving an aggregate of 18% of one
149 lane, for a multiplexing equivalent of 128 samples per lane).

150

151 *2.4 Processing of target capture data*

152 A total of 3,937,346 read pairs from the sample receiving the greatest number of reads were
153 used to *de novo* assemble target sequences for each target region using the assembly by
154 reduced complexity (ARC) pipeline (Hunter et al., 2015). A single assembled contig was
155 selected for each original target region by means of reciprocal best blast hit (RBBH) (Rivera
156 et al., 1998), and these were used as a reference assembly for all downstream analyses.
157 Adapter contamination was removed from sample reads using skewer v0.2.2 (Jiang et al.,
158 2014), and reads were then mapped to the reference assembly using BWA-MEM v0.7.15-
159 r1140 (Li, 2013). Picard tools v2.9.2 (<https://broadinstitute.github.io/picard/>) was used to add
160 read group information and to mark PCR duplicates, and HaplotypeCaller and

161 GenotypeGVCFs from GATK v3.8 (McKenna et al., 2010) were used jointly to genotype the
162 relevant groups of samples (either crested newts or crested newts + marbled newts depending
163 on the analysis; see below). SNPs that failed any of the following hard filters were removed:
164 $QD < 2$, $MQ < 40$, $FS > 60$, $MQRankSum < -12.5$, $ReadPosRankSum < -8$, and $QUAL < 30$
165 (Poplin et al., 2017). We next attempted to remove paralogous targets from our dataset with a
166 Hardy Weinberg Equilibrium (HWE) filter for heterozygote excess. Heterozygote excess p-
167 values were calculated for every SNP using vcftools 0.1.15 (Danecek et al., 2011), and any
168 target containing at least one SNP with a heterozygote excess p-value < 0.05 was removed
169 from downstream analysis. More detail on the processing of the target capture data can be
170 found in Supplementary Text S2.

171

172 *2.5 Phylogenetic analyses*

173 A concatenated maximum likelihood phylogeny was inferred with RAxML version 8.2.11
174 (Stamatakis, 2014) based on an alignment of 133,601 SNPs across 5,866 different targets. We
175 included all 23 *Triturus* individuals in this analysis. For gene-tree summary, ASTRAL v5.6.1
176 (Zhang et al., 2017) was used to estimate the crested newt species-tree from 5,610 gene-trees
177 generated in RAxML. The 21 crested newt samples were assigned species membership, and
178 no marbled newts were included because estimating terminal branch lengths is not possible
179 for species with a single representative. For species-tree estimation, SNAPP v1.3.0 (Bryant et
180 al., 2012) within the BEAST v2.4.8 (Bouckaert et al., 2014) environment was used to infer
181 the crested newt species-tree from single biallelic SNPs randomly selected from each of
182 5,581 post-filtering targets. All three individuals per crested newt species were treated as a
183 single terminal and marbled newts were again excluded given our single exemplar sampling
184 of both species. We also estimated divergence times in SNAPP for the crested newts. The
185 split between *T. carnifex* and *T. macedonicus*, assumed to correspond to the origin of the

186 Adriatic Sea at the end of the Messinian Salinity Crisis 5.33 million years ago, was used as a
187 single calibration point (Arntzen et al., 2007; Wielstra and Arntzen, 2011) to produce a rough
188 estimate of the timing of cladogenesis. A detailed description of our strategy for phylogenetic
189 analyses is available in Supplementary Text S3.

190

191 **3. Results**

192 Samples received a mean of 2,812,980 read pairs (s.d. = 585,815). Enrichment was highly
193 efficient, especially given the large genome size of *Triturus*, with an average of 44.5% of raw
194 reads mapping to the assembled target sequences (s.d. = 2.6%). After removing PCR
195 duplicates, which accounted for an average of 22.6% of mapped reads, the unique read on
196 target rate was 34.4% (s.d. = 1.9%). The 23 samples in the final RAxML alignment contained
197 an average of 10.1% missing data (min = 3.2%, max = 31.8%) after setting genotype calls
198 with GQ scores of less than 20 to missing.

199 The concatenated analysis with RAxML supports a basal bifurcation in *Triturus*
200 between the marbled and crested newts (Fig. 3), consistent with the prevailing view that they
201 are reciprocally monophyletic (Arntzen et al., 2007; Espregueira Themudo et al., 2009;
202 Wielstra et al., 2014). RAxML also recovers each of the crested newt species as
203 monophyletic, validating our decision to collapse the three individuals sampled per species in
204 a single terminal in ASTRAL and SNAPP. Furthermore, all five *Triturus* body builds are
205 recovered as monophyletic (cf. Arntzen et al., 2007; Espregueira Themudo et al., 2009;
206 Wielstra et al., 2014). The greatest intraspecific divergence is observed in *T. carnifex*
207 (Supplementary Text S1; Supplementary Fig. S1; Supplementary Table S2).

208 Phylogenetic inference based on data concatenation with RAxML (Fig. 3), gene-tree
209 summary with ASTRAL (Fig. 4a) and species-tree estimation with SNAPP (Fig. 4b) all
210 recover the same crested newt topology, with a basal bifurcation between the *T. karelinii*-

211 group (NTV = 13; *T. ivanbureschi* as the sister taxon to *T. anatolicus* + *T. karelinii*) and the
212 remaining taxa, which themselves are resolved into the species pairs *T. carnifex* + *T.*
213 *macedonicus* (NTV=14; the *T. carnifex*-group), and *T. cristatus* (NTV=15) + *T. dobrogicus*
214 (NTV=16/17). Despite the rapidity of cladogenesis, we obtain strong branch support for
215 every internal node. Even with the uncertainty in dating given a single biogeographically-
216 derived calibration date, the bifurcation giving rise to the four crested newt species groups (cf.
217 Fig. 1) must have occurred over a relatively short time frame (Fig. 5), reflected by two
218 particularly short, but resolvable internal branches (Fig. 3; Fig. 4).

219 The phylogenomic analyses suggest considerable gene-tree/species-tree discordance in
220 *Triturus*. The normalized quartet score of the ASTRAL tree (Fig. 4a), which reflects the
221 proportion of input gene-tree quartets consistent with the species-tree, is 0.63, indicating a
222 high degree of gene-tree discordance. Furthermore, the only node in the SNAPP tree with a
223 posterior probability below 1.0 (i.e. 0.99) is subtended by a very short branch (Fig. 4b).
224 Consistent with the high level of gene-tree/species-tree discordance, we also found that the
225 full mtDNA-based phylogeny of *Triturus* produced a highly supported, but topologically
226 different, phylogeny (Supplementary Text S3; Supplementary Fig. S2; Wielstra and Arntzen,
227 2011).

228 Considering an NTV count of 12, as observed in the marbled newts as well as the most
229 closely related newt genera, as the ancestral state for *Triturus* (Arntzen et al., 2015; Veith et
230 al., 2018), three sequential single-vertebral additions to NTV along internal branches, and one
231 or two additions along the terminal branch leading to *T. dobrogicus* (in which NTV = 16 and
232 NTV = 17 occur at approximately equal frequency; Arntzen et al., 2015; Wielstra et al., 2016)
233 are required under a parsimony criterion (with either ACCTRAN or DELTRAN optimization)
234 to explain the present-day variation in NTV observed in *Triturus* (Fig. 3). This is the
235 minimum possible number of inferred changes in NTV count required to explain the NTV

236 radiation observed today (Supplementary Fig. S3; Supplementary Text S5). No NTV
237 deletions or reversals are required, implying a linear, stepwise, single-addition scenario for
238 NTV expansion in *Triturus*.

239

240 **4. Discussion**

241 We use a large, transcriptome-derived phylogenomic dataset to construct a phylogenetic
242 hypothesis and study the evolution of ecological and phenotypic diversity within the adaptive
243 radiation of *Triturus* newts. In contrast to previous attempts to recover a multilocus species-
244 tree (Arntzen et al., 2007; Espregueira Themudo et al., 2009; Wielstra et al., 2014), we
245 recover full phylogenetic resolution with strong support across the tree. Despite cladogenesis
246 having occurred in a relatively brief time window (Fig. 5), resulting in a high degree of gene-
247 tree/species-tree discordance, independent phylogenetic approaches based on data
248 concatenation (RAxML), gene-tree summarization (ASTRAL) and species-tree estimation
249 (SNAPP), all recover the same, highly supported topology for *Triturus* (Fig. 3; Fig. 4). Our
250 *Triturus* case study underscores that sequence capture by target enrichment is a promising
251 approach to resolve the phylogenetic challenges associated with adaptive radiations,
252 particularly for taxa with large and complicated genomes where other genomic approaches
253 are impractical, including salamanders (McCartney-Melstad et al., 2016).

254 Our new phylogenetic hypothesis allows us to place the eco-morphological
255 differentiation shown by *Triturus* into a coherent evolutionary context. Over time, *Triturus*
256 expanded its range of NTV to encompass higher counts (Fig. 3). The *Triturus* tree is
257 consistent with a maximally parsimonious scenario, under which four to five character state
258 changes are required to explain the radiation in NTV observed today. Any other possible
259 phylogenetic relationship among *Triturus* body builds would require a higher number of
260 inferred NTV changes (Supplementary Fig. S3). Three of these inferred changes are

261 positioned along internal branches, of which two are particularly short, suggesting that
262 changes in NTV count can evolve over a relatively short time. The fourth and fifth inferred
263 change are situated on the external branch leading to *T. dobrogicus*, the only *Triturus* species
264 with substantial intraspecific variation in NTV count (Arntzen et al., 2015; Wielstra et al.,
265 2016).

266 Newts annually alternate between an aquatic and a terrestrial habitat, and the
267 functional trade-off between adaptation to life in water or on land likely poses contrasting
268 demands on body build (Fish and Baudinette, 1999; Gillis and Blob, 2001; Gvoždík and van
269 Damme, 2006; Shine and Shetty, 2001). Considering the observed relationship between one
270 additional trunk vertebra and an extra month annually spent in the water (Fig. 1), the
271 extraordinary NTV variation observed in *Triturus* may reflect the morphological mechanism
272 by which more efficient exploitation of a wider range in hydroperiod (i.e. the annual
273 availability of standing water) evolved. Despite the evolvability of NTV count (Arntzen et al.,
274 2015), NTV evolution has been phylogenetically constrained in *Triturus*. Apparently the
275 change in NTV was directional and involved the addition of a single trunk vertebra at a time
276 (Fig. 3; Supplementary Fig. S3). Species with a more derived body build, reflected in a
277 higher NTV, have a relatively prolonged aquatic period and, because species with transitional
278 NTV counts remain extant, the end result is an eco-morphological radiation.

279 *Triturus* newts show a slight degree of intraspecific variation in NTV today. Such
280 variation is partially explained by interspecific hybridization (emphasizing the genetic basis
281 of NTV count; Arntzen et al., 2014), but there is standing variation in NTV count within all
282 *Triturus* species (Slijepčević et al., 2015). This suggests that, during *Triturus* evolution, there
283 has always been intraspecific NTV count polymorphism that could be subjected to natural
284 selection. Whether there is a causal relationship between the directional, parsimonious
285 evolution of higher NTV and the equally parsimonious evolutionary increase in aquatic

286 lifestyle, and, if so, which of these two may be the actual target of selection, remain important
287 open questions. A proper understanding of the functional relationship between NTV, body
288 build and fitness in aquatic/terrestrial environments in *Triturus* is still lacking (Gvođík and
289 van Damme, 2006), and functional studies exploring this fitness landscape across intra and
290 interspecific variation in NTV is an important next step in establishing a firm causal
291 relationship between variation, performance and fitness. The recent availability of the first
292 salamander genomes (Elewa et al., 2017; Nowoshilow et al., 2018; Smith et al., 2018) finally
293 offers the prospect of sequencing the genome of each *Triturus* species and exploring the
294 developmental basis for NTV and its functional consequences in the diversification of the
295 genus.

296

297 **Acknowledgements**

298 Andrea Chiochio, Daniele Canestrelli, Michael Fahrbach, Ana Ivanović, Raymond van der
299 Lans, and Kurtuluş Olgun helped obtain samples for transcriptome sequencing. Permits were
300 provided by the Italian Ministry of the Environment (DPN-2009-0026530), the Environment
301 Protection Agency of Montenegro (no. UPI-328/4), the Ministry of Energy, Development and
302 Environmental Protection of Republic of Serbia (no. 353-01-75/2014-08), and TÜBİTAK,
303 Turkey (no. 113Z752). RAVON & Natuurbalans-Limes Divergens provided the *T. carnifex*
304 used to create c0t-1. Tara Luckau helped in the lab. Peter Scott provided valuable suggestions
305 on methodology. Wiesław Babik and Ana Ivanović commented on an earlier version of this
306 manuscript. This work used the Vincent J. Coates Genomics Sequencing Laboratory at UC
307 Berkeley, supported by NIH S10 Instrumentation Grants S10RR029668 and S10RR027303.
308 Computing resources were provided by XSEDE (Towns et al., 2014) and the Texas
309 Advanced Computing Center (TACC) Stampede2 cluster at The University of Texas at
310 Austin.

311

312 **Funding**

313 This project has received funding from the European Union's Horizon 2020 research and
314 innovation programme under the Marie Skłodowska-Curie grant agreement No. 655487.

315

316 **Data availability**

317 Raw sequence read data for the sequence capture libraries of the 23 *Triturus* samples and the
318 12 transcriptome libraries are available at SRA (PRJNA498336). Transcriptome assemblies,
319 genotype calls (VCF) for the 21- and 23-sample datasets, input files for the RAxML,
320 ASTRAL and SNAPP analyses, and synthesized target sequences are available at Zenodo
321 (<https://doi.org/10.5281/zenodo.1470914>). Supplementary data associated with this article
322 can be found, in the online version, at [\[xxx\]](#)

323

324 **References**

- 325 Abdelkrim, J., Aznar-Cormano, L., Fedosov, A., Kantor, Y., Lozouet, P., Phuong, M.,
326 Zaharias, P., Puillandre, N., 2018. Exon-capture based phylogeny and diversification of the
327 venomous gastropods (Neogastropoda, Conoidea). *Mol. Biol. Evol.* 35, 2355–2374.
- 328 Alföldi, J., Di Palma, F., Grabherr, M., Williams, C., Kong, L., Mauceli, E., Russell, P.,
329 Lowe, C.B., Glor, R.E., Jaffe, J.D., Ray, D.A., Boissinot, S., Shedlock, A.M., Botka, C.,
330 Castoe, T.A., Colbourne, J.K., Fujita, M.K., Moreno, R.G., ten Hallers, B.F., Haussler, D.,
331 Heger, A., Heiman, D., Janes, D.E., Johnson, J., de Jong, P.J., Koriabine, M.Y., Lara, M.,
332 Novick, P.A., Organ, C.L., Peach, S.E., Poe, S., Pollock, D.D., de Queiroz, K., Sanger, T.,
333 Searle, S., Smith, J.D., Smith, Z., Swofford, R., Turner-Maier, J., Wade, J., Young, S.,
334 Zadissa, A., Edwards, S.V., Glenn, T.C., Schneider, C.J., Losos, J.B., Lander, E.S., Breen, M.,
335 Ponting, C.P., Lindblad-Toh, K., 2011. The genome of the green anole lizard and a
336 comparative analysis with birds and mammals. *Nature* 477, 587.
- 337 Arntzen, J.W., 2003. *Triturus cristatus* Superspecies - Kammolch-Artenkreis (*Triturus*
338 *cristatus* (Laurenti, 1768) - Nördlicher Kammolch, *Triturus carnifex* (Laurenti, 1768) -
339 Italienischer Kammolch, *Triturus dobrogicus* (Kiritzescu, 1903) - Donau-Kammolch,
340 *Triturus karelinii* (Strauch, 1870) - Südlicher Kammolch). In: Grossenbacher, K., Thiesmeier,
341 B. (Eds.), *Handbuch der Reptilien und Amphibien Europas*. Schwanzlurche IIA. Aula-Verlag,
342 Wiebelsheim, pp. 421-514.

- 343 Arntzen, J.W., Beukema, W., Galis, F., Ivanović, A., 2015. Vertebral number is highly
344 evolvable in salamanders and newts (family Salamandridae) and variably associated with
345 climatic parameters. *Contrib. Zool.* 84, 85-113.
- 346 Arntzen, J.W., Espregueira Themudo, G., Wielstra, B., 2007. The phylogeny of crested newts
347 (*Triturus cristatus* superspecies): nuclear and mitochondrial genetic characters suggest a hard
348 polytomy, in line with the paleogeography of the centre of origin. *Contrib. Zool.* 76, 261-278.
- 349 Arntzen, J.W., Wallis, G.P., 1999. Geographic variation and taxonomy of crested newts
350 (*Triturus cristatus* superspecies): morphological and mitochondrial data. *Contrib. Zool.* 68,
351 181-203.
- 352 Arntzen, J.W., Wielstra, B., Wallis, G.P., 2014. The modality of nine *Triturus* newt hybrid
353 zones, assessed with nuclear, mitochondrial and morphological data. *Biol. J. Linn. Soc.* 113,
354 604–622.
- 355 Bi, K., Vanderpool, D., Singhal, S., Linderoth, T., Moritz, C., Good, J.M., 2012.
356 Transcriptome-based exon capture enables highly cost-effective comparative genomic data
357 collection at moderate evolutionary scales. *BMC Genomics* 13, 403.
- 358 Bork, P., Dandekar, T., Diaz-Lazcoz, Y., Eisenhaber, F., Huynen, M., Yuan, Y., 1998.
359 Predicting function: from genes to genomes and back. *J. Mol. Biol.* 283, 707-725.
- 360 Bouckaert, R., Heled, J., Kühnert, D., Vaughan, T., Wu, C.-H., Xie, D., Suchard, M.A.,
361 Rambaut, A., Drummond, A.J., 2014. BEAST 2: a software platform for Bayesian
362 evolutionary analysis. *PLoS Comput. Biol.* 10, e1003537.
- 363 Bragg, J.G., Potter, S., Bi, K., Moritz, C., 2016. Exon capture phylogenomics: efficacy across
364 scales of divergence. *Mol. Ecol. Resour.* 16, 1059-1068.
- 365 Bryant, D., Bouckaert, R., Felsenstein, J., Rosenberg, N.A., RoyChoudhury, A., 2012.
366 Inferring species trees directly from biallelic genetic markers: bypassing gene trees in a full
367 coalescent analysis. *Mol. Biol. Evol.* 29, 1917-1932.
- 368 Camacho, C., Coulouris, G., Avagyan, V., Ma, N., Papadopoulos, J., Bealer, K., Madden,
369 T.L., 2009. BLAST+: architecture and applications. *BMC Bioinformatics* 10, 421-421.
- 370 Crawford, N.G., Faircloth, B.C., McCormack, J.E., Brumfield, R.T., Winker, K., Glenn, T.C.,
371 2012. More than 1000 ultraconserved elements provide evidence that turtles are the sister
372 group of archosaurs. *Biol. Lett.* 8, 783-786.
- 373 Danecek, P., Auton, A., Abecasis, G., Albers, C.A., Banks, E., DePristo, M.A., Handsaker,
374 R.E., Lunter, G., Marth, G.T., Sherry, S.T., McVean, G., Durbin, R., Genomes Project
375 Analysis, G., 2011. The variant call format and VCFtools. *Bioinformatics* 27, 2156-2158.
- 376 Degnan, J.H., Rosenberg, N.A., 2006. Discordance of species trees with their most likely
377 gene trees. *PLoS Genet.* 2, e68.
- 378 Edgar, R.C., 2010. Search and clustering orders of magnitude faster than BLAST.
379 *Bioinformatics* 26, 2460-2461.

- 380 Elewa, A., Wang, H., Talavera-López, C., Joven, A., Brito, G., Kumar, A., Hameed, L.S.,
381 Penrad-Mobayed, M., Yao, Z., Zamani, N., Abbas, Y., Abdullayev, I., Sandberg, R.,
382 Grabherr, M., Andersson, B., Simon, A., 2017. Reading and editing the *Pleurodeles waltl*
383 genome reveals novel features of tetrapod regeneration. *Nat. Commun.* 8, 2286.
- 384 Espregueira Themudo, G., Wielstra, B., Arntzen, J.W., 2009. Multiple nuclear and
385 mitochondrial genes resolve the branching order of a rapid radiation of crested newts
386 (*Triturus*, Salamandridae). *Mol. Phylogenet. Evol.* 52, 321-328.
- 387 Felsenstein, J., 1978. Cases in which parsimony or compatibility methods will be positively
388 misleading. *Syst. Biol.* 27, 401-410.
- 389 Fish, F.E., Baudinette, R.V., 1999. Energetics of locomotion by the Australian water rat
390 (*Hydromys chrysogaster*): a comparison of swimming and running in a semi-aquatic mammal.
391 *The Journal of Experimental Biology* 202, 353.
- 392 Giarla, T.C., Esselstyn, J.A., 2015. The challenges of resolving a rapid, recent radiation:
393 empirical and simulated phylogenomics of Philippine shrews. *Syst. Biol.* 64, 727-740.
- 394 Gillis, G.B., Blob, R.W., 2001. How muscles accommodate movement in different physical
395 environments: aquatic vs. terrestrial locomotion in vertebrates. *Comparative Biochemistry*
396 *and Physiology Part A: Molecular & Integrative Physiology* 131, 61-75.
- 397 Glenn, T.C., Bayona-Vásquez, N.J., Kieran, T.J., Pierson, T.W., Hoffberg, S.L., Scott, P.A.,
398 Louha, S., Bentley, K.E., Finger Jr., J.W., Troendle, N., Díaz-Jaimes, P., Mauricio, R.,
399 Faircloth, B.C., 2017. Adapterama III: Quadruple-indexed, triple-enzyme RADseq libraries
400 for about \$1USD per Sample (3RAD). *BioRxiv*.
- 401 Gnirke, A., Melnikov, A., Maguire, J., Rogov, P., LeProust, E.M., Brockman, W., Fennell, T.,
402 Giannoukos, G., Fisher, S., Russ, C., Gabriel, S., Jaffe, D.B., Lander, E.S., Nusbaum, C.,
403 2009. Solution hybrid selection with ultra-long oligonucleotides for massively parallel
404 targeted sequencing. *Nat. Biotechnol.* 27, 182.
- 405 Govedarica, P., Cvijanović, M., Slijepčević, M., Ivanović, A., 2017. Trunk elongation and
406 ontogenetic changes in the axial skeleton of *Triturus* newts. *J. Morphol.* 278, 1577-1585.
- 407 Grabherr, M.G., Haas, B.J., Yassour, M., Levin, J.Z., Thompson, D.A., Amit, I., Adiconis, X.,
408 Fan, L., Raychowdhury, R., Zeng, Q., Chen, Z., Mauceli, E., Hacohen, N., Gnirke, A., Rhind,
409 N., di Palma, F., Birren, B.W., Nusbaum, C., Lindblad-Toh, K., Friedman, N., Regev, A.,
410 2011. Full-length transcriptome assembly from RNA-Seq data without a reference genome.
411 *Nat. Biotechnol.* 29, 644-652.
- 412 Gvoždík, L., van Damme, R., 2006. *Triturus* newts defy the running-swimming dilemma.
413 *Evolution* 60, 2110-2121.
- 414 Hammond, S.A., Warren, R.L., Vandervalk, B.P., Kucuk, E., Khan, H., Gibb, E.A., Pandoh,
415 P., Kirk, H., Zhao, Y., Jones, M., Mungall, A.J., Coope, R., Pleasance, S., Moore, R.A., Holt,
416 R.A., Round, J.M., Ohora, S., Walle, B.V., Veldhoen, N., Helbing, C.C., Birol, I., 2017. The
417 North American bullfrog draft genome provides insight into hormonal regulation of long
418 noncoding RNA. *Nat. Commun.* 8, 1433.

- 419 Hellsten, U., Harland, R.M., Gilchrist, M.J., Hendrix, D., Jurka, J., Kapitonov, V.,
420 Ovcharenko, I., Putnam, N.H., Shu, S., Taher, L., Blitz, I.L., Blumberg, B., Dichmann, D.S.,
421 Dubchak, I., Amaya, E., Detter, J.C., Fletcher, R., Gerhard, D.S., Goodstein, D., Graves, T.,
422 Grigoriev, I.V., Grimwood, J., Kawashima, T., Lindquist, E., Lucas, S.M., Mead, P.E.,
423 Mitros, T., Ogino, H., Ohta, Y., Poliakov, A.V., Pollet, N., Robert, J., Salamov, A., Sater,
424 A.K., Schmutz, J., Terry, A., Vize, P.D., Warren, W.C., Wells, D., Wills, A., Wilson, R.K.,
425 Zimmerman, L.B., Zorn, A.M., Grainger, R., Grammer, T., Khokha, M.K., Richardson, P.M.,
426 Rokhsar, D.S., 2010. The genome of the western clawed frog *Xenopus tropicalis*. *Science*
427 328, 633.
- 428 Hunter, S.S., Lyon, R.T., Sarver, B.A.J., Hardwick, K., Forney, L.J., Settles, M.L., 2015.
429 Assembly by Reduced Complexity (ARC): a hybrid approach for targeted assembly of
430 homologous sequences. *bioRxiv*.
- 431 Irisarri, I., Meyer, A., 2016. The identification of the closest living relative(s) of tetrapods:
432 phylogenomic lessons for resolving short ancient internodes. *Syst. Biol.* 65, 1057-1075.
- 433 Jarvis, E.D., Mirarab, S., Aberer, A.J., Li, B., Houde, P., Li, C., Ho, S.Y.W., Faircloth, B.C.,
434 Nabholz, B., Howard, J.T., Suh, A., Weber, C.C., da Fonseca, R.R., Li, J., Zhang, F., Li, H.,
435 Zhou, L., Narula, N., Liu, L., Ganapathy, G., Boussau, B., Bayzid, M.S., Zavidovych, V.,
436 Subramanian, S., Gabaldón, T., Capella-Gutiérrez, S., Huerta-Cepas, J., Rekepalli, B., Munch,
437 K., Schierup, M., Lindow, B., Warren, W.C., Ray, D., Green, R.E., Bruford, M.W., Zhan, X.,
438 Dixon, A., Li, S., Li, N., Huang, Y., Derryberry, E.P., Bertelsen, M.F., Sheldon, F.H.,
439 Brumfield, R.T., Mello, C.V., Lovell, P.V., Wirthlin, M., Schneider, M.P.C., Prosdocimi, F.,
440 Samaniego, J.A., Velazquez, A.M.V., Alfaro-Núñez, A., Campos, P.F., Petersen, B.,
441 Sicheritz-Ponten, T., Pas, A., Bailey, T., Scofield, P., Bunce, M., Lambert, D.M., Zhou, Q.,
442 Perelman, P., Driskell, A.C., Shapiro, B., Xiong, Z., Zeng, Y., Liu, S., Li, Z., Liu, B., Wu, K.,
443 Xiao, J., Yinqi, X., Zheng, Q., Zhang, Y., Yang, H., Wang, J., Smeds, L., Rheindt, F.E.,
444 Braun, M., Fjeldsa, J., Orlando, L., Barker, F.K., Jönsson, K.A., Johnson, W., Koepfli, K.-P.,
445 O'Brien, S., Haussler, D., Ryder, O.A., Rahbek, C., Willerslev, E., Graves, G.R., Glenn, T.C.,
446 McCormack, J., Burt, D., Ellegren, H., Alström, P., Edwards, S.V., Stamatakis, A., Mindell,
447 D.P., Cracraft, J., Braun, E.L., Warnow, T., Jun, W., Gilbert, M.T.P., Zhang, G., 2014.
448 Whole-genome analyses resolve early branches in the tree of life of modern birds. *Science*
449 346, 1320.
- 450 Jiang, H., Lei, R., Ding, S.-W., Zhu, S., 2014. Skewer: a fast and accurate adapter trimmer for
451 next-generation sequencing paired-end reads. *BMC Bioinformatics* 15, 182.
- 452 Kutschera, V.E., Bidon, T., Hailer, F., Rodi, J.L., Fain, S.R., Janke, A., 2014. Bears in a
453 forest of gene trees: phylogenetic inference is complicated by incomplete lineage sorting and
454 gene flow. *Mol. Biol. Evol.* 31, 2004-2017.
- 455 Lanza, B., Arntzen, J.W., Gentile, E., 2010. Vertebral numbers in the Caudata of the Western
456 Palearctic (Amphibia). *Atti Mus. Civ. Stor. Nat. Trieste* 54, 3-114.
- 457 Leaché, A.D., Banbury, B.L., Linkem, C.W., de Oca, A.N.-M., 2016. Phylogenomics of a
458 rapid radiation: is chromosomal evolution linked to increased diversification in north
459 american spiny lizards (Genus *Sceloporus*)? *BMC Evol. Biol.* 16, 63.
- 460 Leaché, A.D., Harris, R.B., Rannala, B., Yang, Z., 2014. The influence of gene flow on
461 species tree estimation: a simulation study. *Syst. Biol.* 63, 17-30.

- 462 L veill -Bourret,  ., Starr, J.R., Ford, B.A., Moriarty Lemmon, E., Lemmon, A.R., 2018.
463 Resolving rapid radiations within angiosperm families using anchored phylogenomics. *Syst.*
464 *Biol.* 67, 94-112.
- 465 Li, H., 2013. Aligning sequence reads, clone sequences and assembly contigs with BWA-
466 MEM. arXiv preprint arXiv:1303.3997.
- 467 Mallet, J., Besansky, N., Hahn, M.W., 2016. How reticulated are species? *Bioessays* 38, 140-
468 149.
- 469 McCartney-Melstad, E., Mount, G.G., Bradley Shaffer, H., 2016. Exon capture optimization
470 in amphibians with large genomes. *Mol. Ecol. Resour.* 16, 1084-1094.
- 471 McCartney-Melstad, E., Vu, J.K., Shaffer, H.B., 2018. Genomic data recover previously
472 undetectable fragmentation effects in an endangered amphibian. *Mol. Ecol.*,
473 <https://doi.org/10.1111/mec.14892>.
- 474 McCormack, J.E., Faircloth, B.C., Crawford, N.G., Gowaty, P.A., Brumfield, R.T., Glenn,
475 T.C., 2012. Ultraconserved elements are novel phylogenomic markers that resolve placental
476 mammal phylogeny when combined with species-tree analysis. *Genome Res.* 22, 746-754.
- 477 McKenna, A., Hanna, M., Banks, E., Sivachenko, A., Cibulskis, K., Kernytsky, A., Garimella,
478 K., Altshuler, D., Gabriel, S., Daly, M., DePristo, M.A., 2010. The Genome Analysis Toolkit:
479 A MapReduce framework for analyzing next-generation DNA sequencing data. *Genome Res.*
480 20, 1297-1303.
- 481 Meiklejohn, K.A., Faircloth, B.C., Glenn, T.C., Kimball, R.T., Braun, E.L., 2016. Analysis of
482 a rapid evolutionary radiation using ultraconserved elements: evidence for a bias in some
483 multispecies coalescent methods. *Syst. Biol.* 65, 612-627.
- 484 Meilink, W.R.M., Arntzen, J.W., van Delft, J.J.C.W., Wielstra, B., 2015. Genetic pollution of
485 a threatened native crested newt species through hybridization with an invasive congener in
486 the Netherlands. *Biol. Conserv.* 184, 145-153.
- 487 Nater, A., Burri, R., Kawakami, T., Smeds, L., Ellegren, H., 2015. Resolving evolutionary
488 relationships in closely related species with whole-genome sequencing data. *Syst. Biol.* 64,
489 1000-1017.
- 490 Neves, L.G., Davis, J.M., Barbazuk, W.B., Kirst, M., 2013. Whole-exome targeted
491 sequencing of the uncharacterized pine genome. *The Plant Journal* 75, 146-156.
- 492 Nowoshilow, S., Schloissnig, S., Fei, J.-F., Dahl, A., Pang, A.W.C., Pippel, M., Winkler, S.,
493 Hastie, A.R., Young, G., Roscito, J.G., Falcon, F., Knapp, D., Powell, S., Cruz, A., Cao, H.,
494 Habermann, B., Hiller, M., Tanaka, E.M., Myers, E.W., 2018. The axolotl genome and the
495 evolution of key tissue formation regulators. *Nature* 554, 50-55.
- 496 Pamilo, P., Nei, M., 1988. Relationships between gene trees and species trees. *Mol. Biol.*
497 *Evol.* 5, 568-583.
- 498 Philippe, H., Brinkmann, H., Lavrov, D.V., Littlewood, D.T.J., Manuel, M., W rheide, G.,
499 Baurain, D., 2011. Resolving difficult phylogenetic questions: why more sequences are not
500 enough. *PLoS Biol.* 9, e1000602.

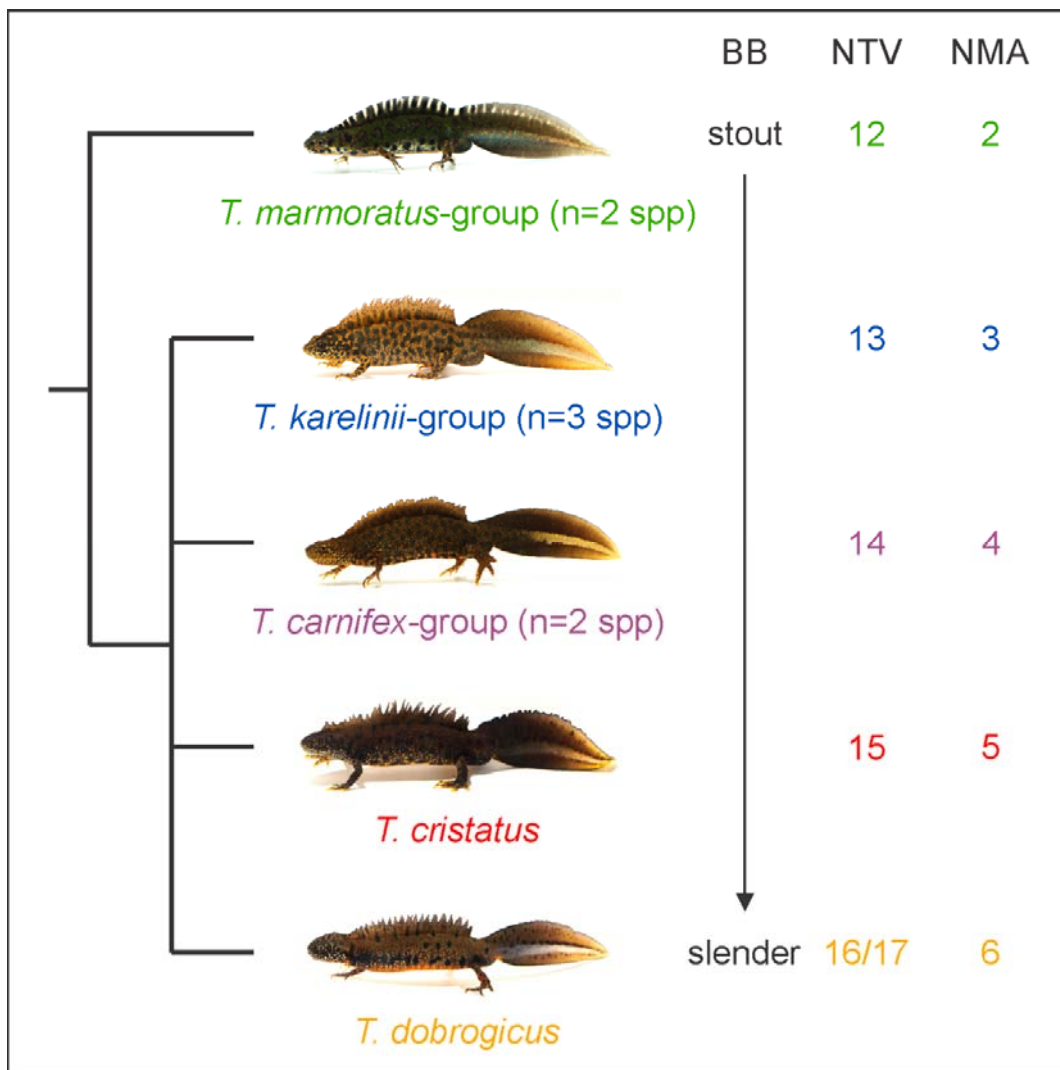
- 501 Pollard, D.A., Iyer, V.N., Moses, A.M., Eisen, M.B., 2006. Widespread discordance of gene
502 trees with species tree in *Drosophila*: evidence for incomplete lineage sorting. *PLoS Genet.* 2,
503 e173.
- 504 Poplin, R., Ruano-Rubio, V., DePristo, M.A., Fennell, T.J., Carneiro, M.O., Van der Auwera,
505 G.A., Kling, D.E., Gauthier, L.D., Levy-Moonshine, A., Roazen, D., Shakir, K., Thibault, J.,
506 Chandran, S., Whelan, C., Lek, M., Gabriel, S., Daly, M.J., Neale, B., MacArthur, D.G.,
507 Banks, E., 2017. Scaling accurate genetic variant discovery to tens of thousands of samples.
508 bioRxiv.
- 509 Rivera, M.C., Jain, R., Moore, J.E., Lake, J.A., 1998. Genomic evidence for two functionally
510 distinct gene classes. *Proc. Natl. Acad. Sci. U.S.A.* 95, 6239-6244.
- 511 Sambrook, J., Russell, D.W., 2001. *Molecular cloning: a laboratory manual* 3rd edition.
512 ColdSpring-Harbour Laboratory Press, UK.
- 513 Scott, P.A., Glenn, T.C., Rissler, L.J., 2018. Resolving taxonomic turbulence and uncovering
514 cryptic diversity in the musk turtles (*Sternotherus*) using robust demographic modeling. *Mol.*
515 *Phylogenet. Evol.* 120, 1-15.
- 516 Shaffer, H.B., Minx, P., Warren, D.E., Shedlock, A.M., Thomson, R.C., Valenzuela, N.,
517 Abramyan, J., Amemiya, C.T., Badenhorst, D., Biggar, K.K., Borchert, G.M., Botka, C.W.,
518 Bowden, R.M., Braun, E.L., Bronikowski, A.M., Bruneau, B.G., Buck, L.T., Capel, B.,
519 Castoe, T.A., Czerwinski, M., Delehaunty, K.D., Edwards, S.V., Fronick, C.C., Fujita, M.K.,
520 Fulton, L., Graves, T.A., Green, R.E., Haerty, W., Hariharan, R., Hernandez, O., Hillier,
521 L.W., Holloway, A.K., Janes, D., Janzen, F.J., Kandath, C., Kong, L., de Koning, A.J., Li, Y.,
522 Litterman, R., McGaugh, S.E., Mork, L., O'Laughlin, M., Paitz, R.T., Pollock, D.D., Ponting,
523 C.P., Radhakrishnan, S., Raney, B.J., Richman, J.M., St John, J., Schwartz, T., Sethuraman,
524 A., Spinks, P.Q., Storey, K.B., Thane, N., Vinar, T., Zimmerman, L.M., Warren, W.C.,
525 Mardis, E.R., Wilson, R.K., 2013. The western painted turtle genome, a model for the
526 evolution of extreme physiological adaptations in a slowly evolving lineage. *Genome Biol.*
527 14, R28.
- 528 Shi, C.-M., Yang, Z., 2018. Coalescent-based analyses of genomic sequence data provide a
529 robust resolution of phylogenetic relationships among major groups of gibbons. *Mol. Biol.*
530 *Evol.* 35, 159-179.
- 531 Shine, R., Shetty, S., 2001. Moving in two worlds: aquatic and terrestrial locomotion in sea
532 snakes (*Laticauda colubrina*, Laticaudidae). *J. Evol. Biol.* 14, 338-346.
- 533 Slijepčević, M., Galis, F., Arntzen, J.W., Ivanović, A., 2015. Homeotic transformations and
534 number changes in the vertebral column of *Triturus* newts. *PeerJ* 3, e1397.
- 535 Smith, J.J., Timoshevskaya, N., Timoshevskiy, V.A., Keinath, M.C., Hardy, D., Voss, S.R.,
536 2018. A chromosome-scale assembly of the enormous (32 Gb) *Axolotl* genome. bioRxiv.
- 537 Song, S., Liu, L., Edwards, S.V., Wu, S., 2012. Resolving conflict in eutherian mammal
538 phylogeny using phylogenomics and the multispecies coalescent model. *Proc. Natl. Acad. Sci.*
539 *U.S.A.* 109, 14942-14947.

- 540 Spinks, P.Q., Thomson, R.C., Pauly, G.B., Newman, C.E., Mount, G., Shaffer, H.B., 2013.
541 Misleading phylogenetic inferences based on single-exemplar sampling in the turtle genus
542 *Pseudemys*. Mol. Phylogenet. Evol. 68, 269-281.
- 543 Stamatakis, A., 2014. RAxML version 8: a tool for phylogenetic analysis and post-analysis of
544 large phylogenies. Bioinformatics 30, 1312-1313.
- 545 Stroud, J.T., Losos, J.B., 2016. Ecological opportunity and adaptive radiation. Annu. Rev.
546 Ecol. Evol. Syst. 47, 507-532.
- 547 Sun, Y.-B., Xiong, Z.-J., Xiang, X.-Y., Liu, S.-P., Zhou, W.-W., Tu, X.-L., Zhong, L., Wang,
548 L., Wu, D.-D., Zhang, B.-L., Zhu, C.-L., Yang, M.-M., Chen, H.-M., Li, F., Zhou, L., Feng,
549 S.-H., Huang, C., Zhang, G.-J., Irwin, D., Hillis, D.M., Murphy, R.W., Yang, H.-M., Che, J.,
550 Wang, J., Zhang, Y.-P., 2015. Whole-genome sequence of the Tibetan frog *Nanorana parkeri*
551 and the comparative evolution of tetrapod genomes. Proc. Natl. Acad. Sci. U.S.A. 112, E1257.
- 552 Swofford, D.L., Waddell, P.J., Huelsenbeck, J.P., Foster, P.G., Lewis, P.O., Rogers, J.S.,
553 2001. Bias in phylogenetic estimation and Its relevance to the choice between parsimony and
554 likelihood methods. Syst. Biol. 50, 525-539.
- 555 Tatusov, R.L., Koonin, E.V., Lipman, D.J., 1997. A genomic perspective on protein families.
556 Science 278, 631.
- 557 Towns, J., Cockerill, T., Dahan, M., Foster, I., Gaither, K., Grimshaw, A., Hazlewood, V.,
558 Lathrop, S., Lifka, D., Peterson, G.D., Roskies, R., Scott, J.R., Wilkins-Diehr, N., 2014.
559 XSEDE: accelerating scientific discovery. Computing in Science & Engineering 16, 62-74.
- 560 Urošević, A., Slijepčević, M.D., Arntzen, J.W., Ivanović, A., 2016. Vertebral shape and body
561 elongation in *Triturus* newts. Zoology 119, 439-446.
- 562 Veith, M., Bogaerts, S., Pasmans, F., Kieren, S., 2018. The changing views on the
563 evolutionary relationships of extant Salamandridae (Amphibia: Urodela). PLoS ONE 13,
564 e0198237.
- 565 Vukov, T.D., Sotiropoulos, K., Wielstra, B., Džukić, G., Kalezić, M.L., 2011. The evolution
566 of the adult body form of the crested newt (*Triturus cristatus* superspecies, Caudata,
567 Salamandridae). Journal of Zoological Systematics and Evolutionary Research 49, 324-334.
- 568 Whitfield, J.B., Lockhart, P.J., 2007. Deciphering ancient rapid radiations. Trends Ecol. Evol.
569 22, 258-265.
- 570 Wielstra, B., Arntzen, J.W., 2011. Unraveling the rapid radiation of crested newts (*Triturus*
571 *cristatus* superspecies) using complete mitogenomic sequences. BMC Evol. Biol. 11, 162.
- 572 Wielstra, B., Arntzen, J.W., van der Gaag, K., Pabijan, M., Babik, W., 2014. Data
573 concatenation, Bayesian concordance and coalescent-based analyses of the species tree for
574 the rapid radiation of *Triturus* newts. PLoS ONE 9, e111011.
- 575 Wielstra, B., Burke, T., Butlin, R.K., Arntzen, J.W., 2017a. A signature of dynamic
576 biogeography: enclaves indicate past species replacement. Proc. Royal Soc. B 284, 20172014.

- 577 Wielstra, B., Burke, T., Butlin, R.K., Avci, A., Üzümlü, N., Bozkurt, E., Olgun, K., Arntzen,
578 J.W., 2017b. A genomic footprint of hybrid zone movement in crested newts. *Evolution*
579 *Letters* 1, 93-101.
- 580 Wielstra, B., Crnobrnja-Isailović, J., Litvinchuk, S.N., Reijnen, B.T., Skidmore, A.K.,
581 Sotiropoulos, K., Toxopeus, A.G., Tzankov, N., Vukov, T., Arntzen, J.W., 2013. Tracing
582 glacial refugia of *Triturus* newts based on mitochondrial DNA phylogeography and species
583 distribution modeling. *Front. Zool.* 10, 13.
- 584 Wielstra, B., Vörös, J., Arntzen, J.W., 2016. Is the Danube crested newt *Triturus dobrogicus*
585 polytypic? A review and new nuclear DNA data. *Amphib.-Reptil.* 37, 167-177.
- 586 Zhang, C., Sayyari, E., Mirarab, S., 2017. ASTRAL-III: Increased Scalability and Impacts of
587 Contracting Low Support Branches. In: Meidanis, J., Nakhleh, L. (Eds.), *Comparative*
588 *Genomics*. Springer International Publishing, Cham, pp. 53-75.
- 589

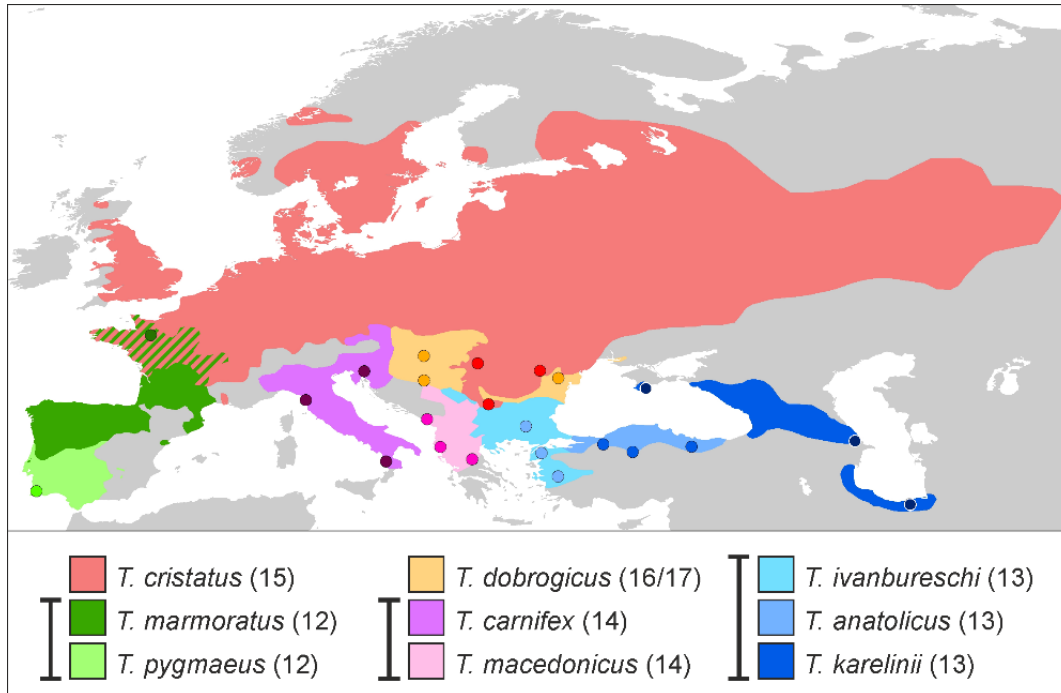
590 **Figures**

591



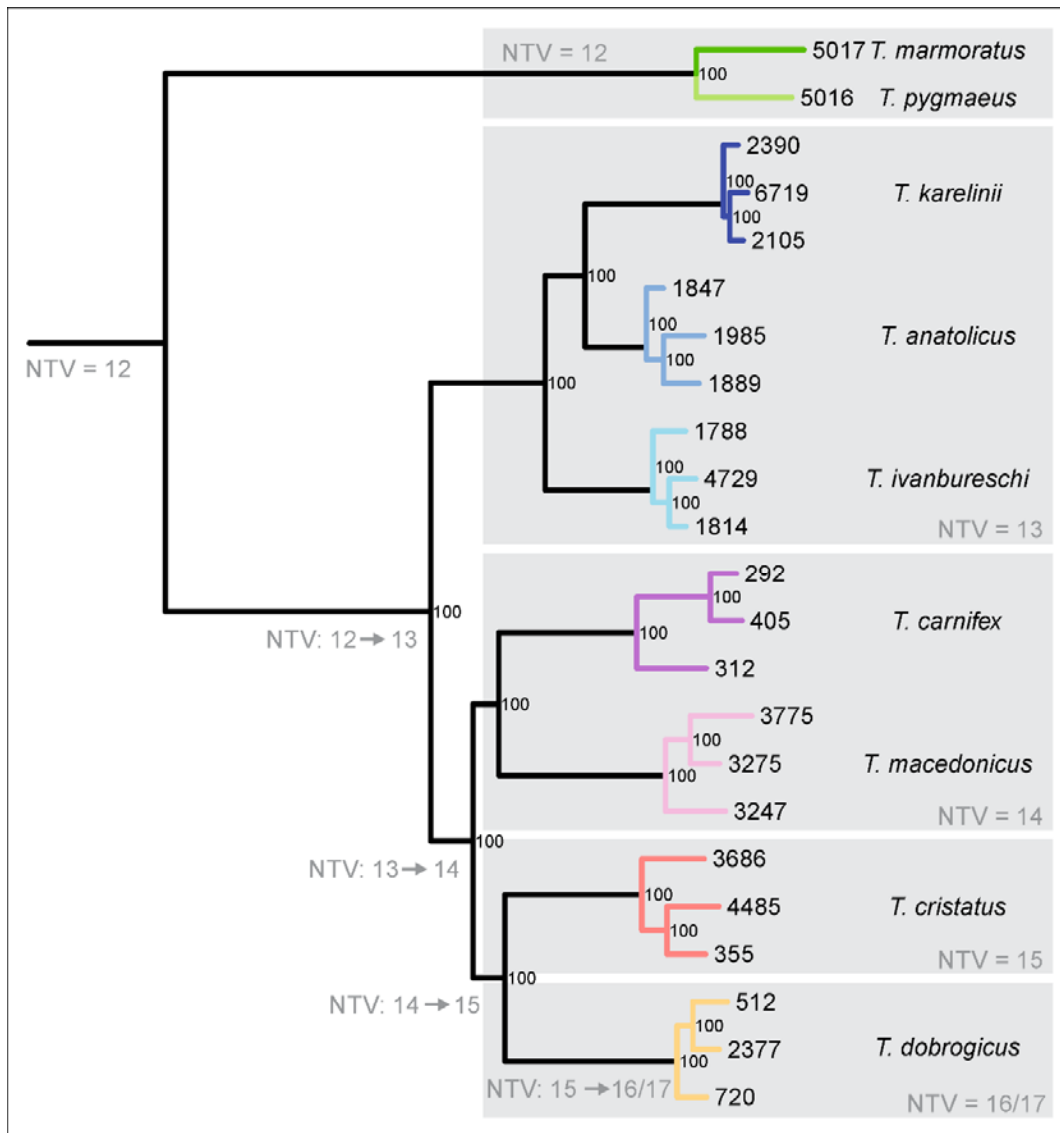
592

593 **Fig. 1. The adaptive radiation of *Triturus* newts.** Five body builds (BB) from stout to
 594 slender are observed in *Triturus* that are also characterized by an increasing number of trunk
 595 vertebrae (NTV) and number of annual aquatic months (NMA). The marbled newts (*T.*
 596 *marmoratus*-group) and crested newts (remaining four BBs) are sister clades. Relationships
 597 among the crested newts are not yet resolved and are the main focus of the present study.



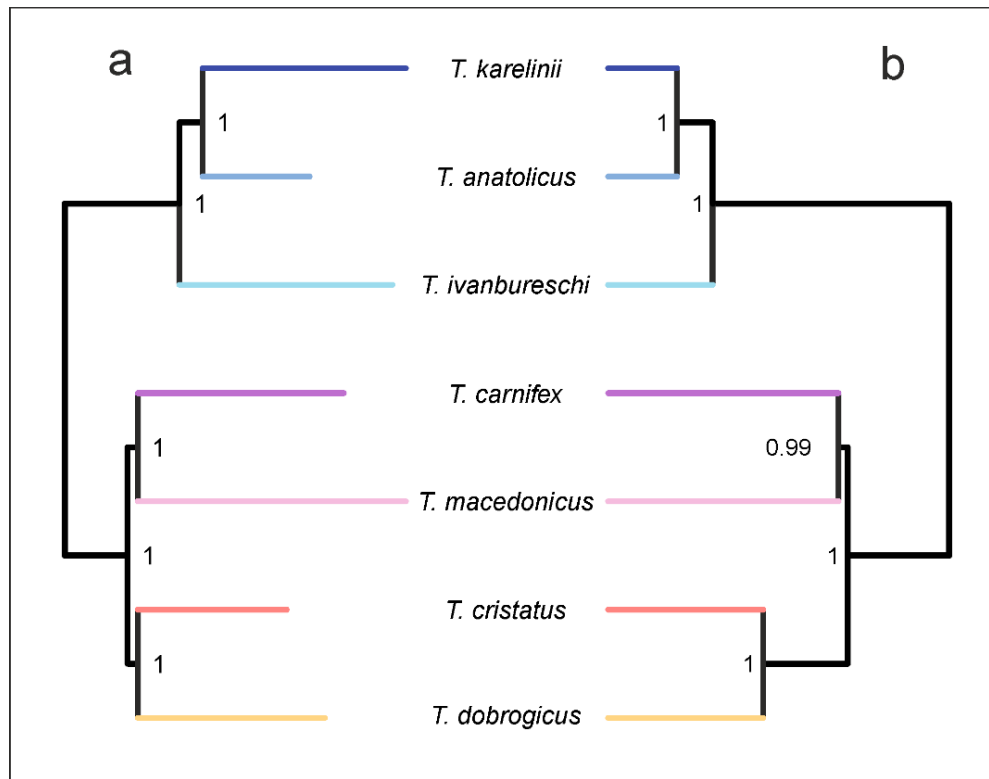
598

599 **Fig. 2. Distribution and sampling scheme for *Triturus*.** Dots represent sample localities
600 (details in Supplementary Table S1). For the marbled newts (in green) a single individual is
601 sampled for each of the two species and for the crested newts (other colours) three
602 individuals are sampled for all seven species. The number in parentheses reflects each species'
603 characteristic number of trunk vertebrae and whiskers link species that possess the same body
604 build (see Fig. 1).



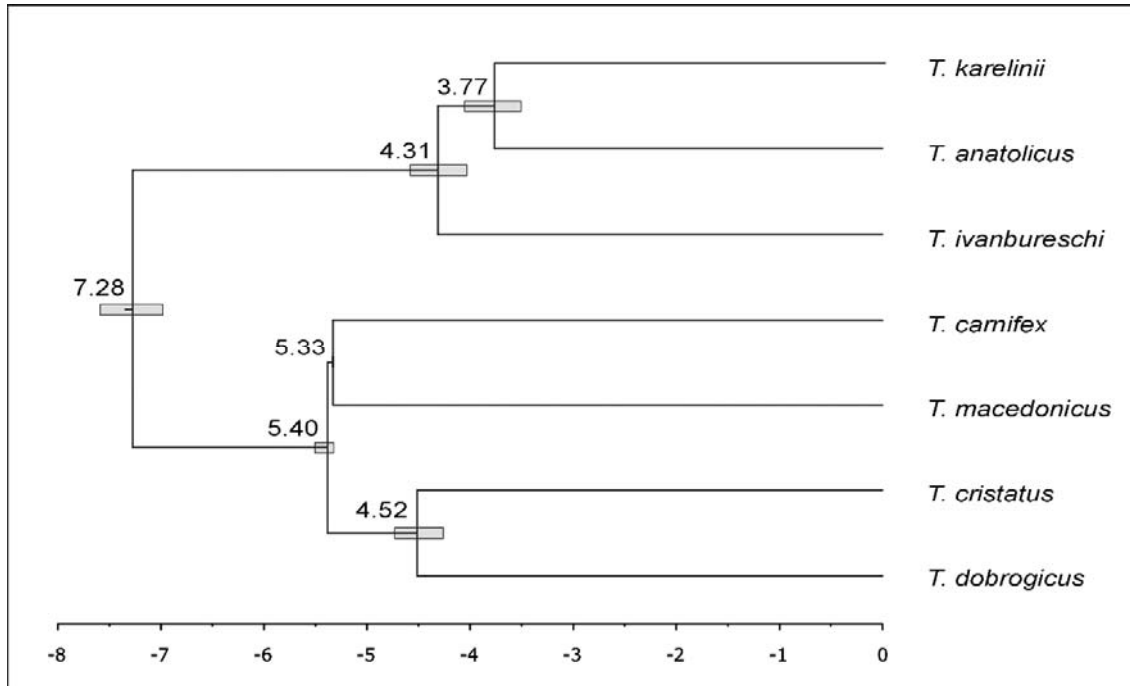
605

606 **Fig. 3. *Triturus* newt phylogeny based on data concatenation with RAxML.** This
 607 maximum likelihood phylogeny is based on 133,601 SNPs derived from 5,866 nuclear
 608 markers. Numbers at nodes indicate bootstrap support from 100 rapid bootstrap replicates.
 609 The five *Triturus* body builds (see Fig. 1) are delineated by grey boxes, with their
 610 characteristic number of trunk vertebrae (NTV) noted. Inferred changes in NTV under the
 611 parsimony criterion are noted along branches. Colours reflect species and correspond to Fig.
 612 2. Tip labels correspond to Supplementary Table S1.



613

614 **Fig. 4. Crested newt phylogeny based on gene-tree summary with ASTRAL and species-**
615 **tree estimation with SNAPP.** The ASTRAL tree (a) is based on 5,610 gene-trees. Numbers
616 at nodes indicate local quartet support posterior probabilities. The SNAPP tree (b) is based on
617 single biallelic SNPs taken from 5,581 nuclear markers. Numbers at nodes indicate posterior
618 probabilities. Colours reflect species and correspond to Fig. 2. Note that both topologies are
619 identical to the phylogeny based on data concatenation (Fig. 3).



620

621 **Fig. 5. Dated species-tree for the crested newts.** Divergence times were determined with

622 SNAPP, using a single *T. carnifex*–*T. macedonicus* inferred split date of 5.33 million years

623 ago as a calibration point. Numbers at nodes reflect median divergence times in millions of

624 years ago and bars the 95% credibility interval around the median.